Rock and Soil Mechanics

Volume 41 | Issue 5 Article 9

10-13-2020

# Prediction and classification of rock mass boreability in TBM tunnel

Xin-lin WU
*Key Laboratory of Geotechnical and Structural Engineering Safety of Hubei Province, Wuhan University, Wuhan, Hubei 430072, China;*

Xiao-ping ZHANG
*Key Laboratory of Geotechnical and Structural Engineering Safety of Hubei Province, Wuhan University, Wuhan, Hubei 430072, China;*, jxhkzhang@163.com

Quan-sheng LIU
*Key Laboratory of Geotechnical and Structural Engineering Safety of Hubei Province, Wuhan University, Wuhan, Hubei 430072, China;*

Wei-wei LI
*Manufacturing and Installation Branch Sinohyaro Bureau 3 Co., Ltd, Xi'an, Shaanxi 710024, China*

*See next page for additional authors*



## Custom Citation

WU Xin-lin, ZHANG Xiao-ping, LIU Quan-sheng, LI Wei-wei, HUANG Ji-min, . Prediction and classification of rock mass boreability in TBM tunnel[J]. Rock and Soil Mechanics, 2020, 41(5): 1721-1729.

Rock and Soil Mechanics 2020 41(5): 1721−1729 ISSN 1000−7598
https: //doi.org/10.16285/j.rsm.2019.5963 rocksoilmech.researchcommons.org/journal

# Prediction and classification of rock mass boreability in TBM tunnel

WU Xin-lin[1, 2], ZHANG Xiao-ping[1, 2], LIU Quan-sheng[1, 2], LI Wei-wei[3], HUANG Ji-min[3]

1. School of Civil Engineering, Wuhan University, Wuhan, Hubei 430072, China;

2. Key Laboratory of Geotechnical and Structural Engineering Safety of Hubei Province, Wuhan University, Wuhan, Hubei 430072, China;

3. Manufacturing and Installation Branch Sinohyaro Bureau 3 Co., Ltd, Xi'an, Shaanxi 710024, China

**Abstract:** Due to the extremely high sensitivity of tunnel boring machine（TBM）performance to rock mass conditions and its huge early investment, it is of great value to evaluate the rock mass boreability and predict the TBM performance. In this study, about 300 sets of field data from China and Iran are collected, covering three different rock types and 5 TBM tunnels. FPI (field penetration index) is selected as the evaluation index of rock mass boreability. Specifically, the relationships between rock uniaxial compressive strength(UCS), rock mass integrity index $K_v$ , angle between main structural plane of rock mass and axis of the tunnel $\alpha$, tunnel diameter, $D$ and rock mass boreability are systematically analyzed. In addition, a unified approach of rock mass parameters which is suitable for the study of rock mass boreability is discussed in detail, and an empirical prediction model of rock mass boreability with relatively high accuracy ( $R^2 = 0.768$) is further established. Based on this model and supplemented by K-center clustering method, the boreability of rock mass are classified into 6 groups, which are then applied to the exploration of the distribution of average cutter thrust and cutterhead rotation speed under various of rock mass boreability conditions. The findings in our work shed light on the evaluation of rock mass boreability, the selection of operational parameters as well as the arrangement of TBM tunnel construction schedule.

**Keywords:** tunnel boring machine(TBM); boreability prediction; rock mass classification; operational parameters

## 1 Introduction

With the development of mechanical manufacturing technology and tunneling industry, full-section hard rock tunnel boring machine (TBM) has been widely used in the construction of super long tunnels [1]. Compared with the traditional drilling and blasting methods, TBM has many advantages such as rapid, safe, economic and environmentally-friendly. However it is also extremely sensitive to the change of rock mass conditions[2]. Under favorable conditions of rock mass boreability, TBM can often yield an ideal penetration rate[3]. Once a hard and intact rock mass with poor boreability is encountered, it is more likely to cause adverse consequences such as high tool wear and low tunneling efficiency[4], resulting in serious delays of engineering progress and economic losses. Due to the huge investments on the early stage of TBM, accurate assessment of rock mass boreability and prediction of TBM tunneling performance are crucial for the selection of construction method, arrangement of construction schedule as well as the control of cost. Therefore, the prediction and evaluation of the boreability of TBM rock mass have long been an important research topic in the field of TBM tunnel construction[5].

In the last four decades, different models for predicting the boreability of TBM rock mass have been proposed by many scholars, which are mainly divided into theoretical models and empirical models[6]. The theoretical models are mainly based on the mechanism of single-cutter rock breaking, and are established through experimental and theoretical analysis of the stress of single cutter. The famous theoretical model (CSM model) of Colorado Institute of Mining and Technology[7] is not capable in the representation of the influence of engineering rock mass discontinuity on TBM tunneling.

In contrast, empirical models are based on the measured parameters of rock mass and rock mass boreability indicators. Through the establishment of empirical models, the TBM rock mass boreability can be predicted. These models include $Q_{TBM}$ model obtained from the improved Q classification of rock mass[8–9], PR model used in the prediction of net penetration rate[10–11], models that predict the field penetration index, FPI[5, 12–18] and NTNU models[19]. Many scholars have also put forward the corresponding classification schemes of rock mass boreability according to the prediction models[5, 8, 12, 16]. However, empirical models are often built on the field data from one or a few tunnels, thus their applications are limited to the projects with similar rock mass conditions. In order to improve the adaptability of the models, it is imperative

Received: 4 July 2019 Revised: 16 September 2019
This work was supported by the National Natural Science Foundation of China (No. 51978541, No. 41941018, No. 51839009).
First author: WU Xin-lin, male, born in 1996, Master degree candidate, focusing on research on rock mass classification of tunnel constructed by TBM. E-mail：2013301550088@whu.edu.cn
Correspongding: ZHANG Xiao-ping, male, born in 1982, PhD, Professor, PhD tutor, research interests: rock mechanics, engineering geology and underground engineering. E-mail: jxhkzhang@ 163. com

to make use of relevant engineering data as much as possible to build a more universally applicable empirical model, as well as an appropriate classification scheme for rock mass boreability.

This study focuses on the field monitoring data of 5 TBM tunnels from China and Iran. The main impact factors for TBM rock mass boreability were analyzed, and the empirical method which is capable in the prediction of TBM rock mass boreability was established. In addition, the classification of TBM rock mass boreability was conducted. The corresponding research results provide guidance in the assessment of rock mass boreability, the selection of TBM tunneling parameters and the arrangement of construction schedule.

## 2 Engineering project and database development

### 2.1 Project profile

This study is based on the field monitoring data collected from 5 TBM construction tunnels from China and Iran. The main technical parameters of TBM are presented in Table 1. Table 2 displays the geological conditions for each tunnel. In the database, the TBM tunnels cut through three types of rock mass, namely igneous rock, sedimentary rock and metamorphic rock. The uniaxial compressive strength of the rock ranges from 25 MPa to 150 MPa.

**Table 1 Specifications of TBMs**

| Project ID | Project | TBM type | Cutterhead diameter/ m | Cutter number | Machine weight/ t | TBM total weight / t | Cutter spacing/ mm | Maximum thrust / kN | Rotational speed of cutterhead / rpm |
|---|---|---|---|---|---|---|---|---|---|
| 1 | Karaj water delivery tunnel[20] | double shield | 4.66 | 31 | — | — | 70(90[15]) | 16 913 | 0–11.00 |
| 2 | Zagroswater delivery tunnel（Section 1[14]and Section 2[13]） | double shield | 6.73 | 42 | — | — | 90 | 28 134 | 0–11.00(9) |
| 3 | West Qinling Tunnel of Lanzhou-Chongqing Railway[21–24] | open | 10.20 | 68 | 800 | — | — | 19 000 | 0–6.32 |
| 4 | A typical diversion tunnel[16] | open | 8.50 | 49 | ~825 | ~1 375 | 89 | 18 769 | 0–6.90 |
| 5 | Yinsong water supply project[25] | open | 7.93(8.03) | 52 | ~650 | ~1 320 | — | 23 560 | 0–7.60 |

Note: The data in brackets are reported in some literature, which are not accepted in this paper.

**Table 2 Geological characteristics of tunneling projects**

| Project | Length of tunnel / km | Lithology | Maximum depth/ m | UCS / MPa |
|---|---|---|---|---|
| Karaj water delivery tunnel [20] | 15.90 | Tuff, shale, sandy tuff | 600 | 30–150 |
| Zagroswater delivery tunnel（Section 1[14]and Section 2[13]） | 26.00 | Limestone, shale, marl limestone, calcareous shale | 650 | 25–150 |
| West Qinling Tunnel of Lanzhou-Chongqing Railway[21–24] | 28.20 | Phyllite, limestone, sandy phyllite | 1 400 | 33–80 |
| A typical diversion tunnel[16] | — | Quartz monosite, granodiorite, monosite | — | 45–115 |
| Yinsong Water supply project[25] | 69.85 | Sandstone, granite, andesite, diorite, tuff, limestone | — | 45–145 |

Note: UCS is uniaxial compressive strength of rock.

### 2.2 Database development

The database mainly includes three categories of parameters, such as mechanical parameters, evaluation indexes of TBM rock mass boreability and rock mass parameters. Among them, the mechanical parameters include the number of cutter $N$, the total thrust of disc cutter TF, TBM cutter rotational speed RPM, etc., which are obtained according to the field records during the construction process.

The evaluation index of TBM rock mass boreability includes penetration rate $\mathrm{PR_{ev}}$ [12], net penetration rate PR[12], and field penetration index, FPI [26], etc. The calculation formulas are as follows:

$$\mathrm{PR}=\frac{L}{T_\mathrm{b}} \tag{1}$$

$$\mathrm{PR_{ev}}=\frac{1\,000\mathrm{PR}}{60\mathrm{RPM}} \tag{2}$$

$$\mathrm{FPI}=\frac{F_\mathrm{n}}{\mathrm{PR_{ev}}} \tag{3}$$

where $L$ is the TBM continuous excavation distance (m); $T_\mathrm{b}$ is the continuous excavation time(h); $\mathrm{PR_{ev}}$ is the penetrate rate, indicating the depth at which the disc cutter cuts into the rock mass per turn(mm/r); and $F_\mathrm{n}$ is the average single cutter thrust(kN), which is estimated by the ratio of total thrust to the number of the cutters on cutterhead $F_\mathrm{n}=\mathrm{TF}/N$ .

In the above evaluation indexes of boreability, under the same rock mass condition, TBM specifications, mechanical parameters and penetration parameters (thrust and rotational speed) exert significant influences on the values of $\mathrm{PR_{ev}}$ and PR. Although the FPI value is still affected by TBM specifications and mechanical parameters, it eliminates the influence of penetration parameters (thrust and rotational speed) to a certain extent, and has been widely applied in the evaluation of rock mass boreability. Therefore, FPI is selected in this paper to characterize the boreability of rock mass. In general, the smaller the FPI, the smaller the thrust required for TBM to reach the specified penetration rate, and the better the boreability of rock mass. The larger the FPI, the worse the boreability of rock mass.

Rock mass parameters include rock uniaxial compressive strength UCS, rock quality designation RQD, intactness degree of rock masses $K_\mathrm{v}$ , angle between tunnel structural plane and tunnel axis $\alpha$, tunnel diameter $D$, groundwater flux $Q$, tunnel buried depth $H$, etc. Due to the difference of geological survey methods between industries and regions, the parameters representing the properties of rock mass in different engineering projects are not identical. In order to facilitate the follow-up research, it is necessary to consider the correlation between different rock mass indexes and unify the rock mass property evaluation index.

Both RQD and $K_v$ are essentially the indicators representing the integrity of rock mass[27]. Based on the research results of previous scholars, the author finds that RQD and $K_v$ are significantly correlated to each other[28–29] (Fig. 1). The *Code for Investigation of Geotechnical Engineering* (GB50021-2001)[30] divides rock mass integrity into five levels based on $K_v$, and divides rock quality into five levels based on RQD. For the convenience of this study, based on the classification results, the author unifies RQD and $K_v$ in the database by referring to Table 3. As is illustrated in Fig. 2, the index representing the integrity of rock mass before and after the conversion is basically consistent with the index of rock mass boreability, showing that this conversion between RQD and $K_v$ is validated in this study. It should be noted that this study only verifies the applicability of the conversion method in Table 3 from the perspective that RQD and $K_v$ are correlated closely to FPI before and after the conversion. Therefore, this conversion method is only applicable in the research on the boreability of TBM rock mass, The more universally applicable conversion method between RQD and $K_v$ should take into account more measured data. Based on the above discussion, the rock mass parameters in this study can be unified. After the unification, the database used in this study contains about 300 groups of valid data from 5 TBM construction tunnels. Due to the incomeplete data collected in each tunnel, some missing data are excluded from the research scope of this study. The descriptive statistics of each parameter in the database are shown in Table 4.

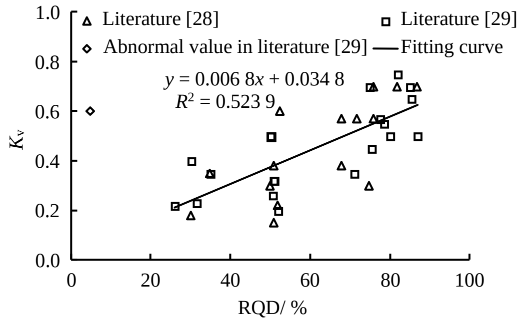


**Fig.1 Relationship between RQD and $K_v$**

**Table 3 Corresponding table between RQD and $K_v$**

| Evaluation index | RQD | $K_v$ |
|---|---|---|
| Intact (excellent) | >90 | >0.75 |
| Fair intact (good) | 75–90 | 0.55–0.75 |
| Fair broken (not good) | 50–75 | 0.35–0.55 |
| Broken (poor) | 25–50 | 0.15–0.35 |
| Highly broken (very poor) | <25 | <0.15 |

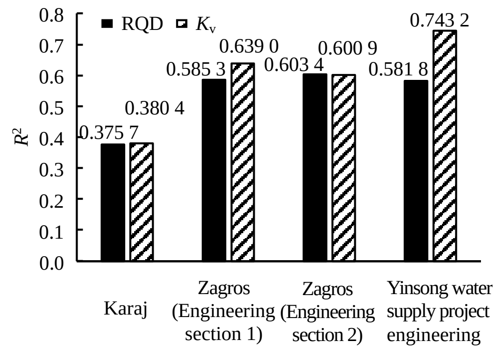


**Fig.2 Correlation coefficient between RQD (or $K_v$) and FPI**

**Table 4 Descriptive statistics of the variables in database**

| Variable | UCS / MPa | $K_v$ | $\alpha$ / (°) | PR / (m • h$^{-1}$) | $PR_{ev}$ / (mm • r$^{-1}$) | FPI / (kN • r • mm$^{-1}$) | $Q$ /(10$^{-1}$L • min$^{-1}$ • m$^{-1}$) | $H$ / m | $F_n$ / kN | RPM / (r • min$^{-1}$) |
|---|---|---|---|---|---|---|---|---|---|---|
| Sample size | 276.00 | 276.00 | 225.00 | 235.00 | 254.00 | 313.00 | 98.00 | 49.00 | 254.00 | 176.00 |
| Range | 135.26 | 0.94 | 82.00 | 4.53 | 14.93 | 80.87 | 22.00 | 291.00 | 264.24 | 3.94 |
| Minimum | 15.24 | 0.06 | 0.00 | 0.74 | 1.77 | 5.80 | 3.00 | 110.00 | 76.26 | 3.56 |
| Maximum | 150.50 | 1.00 | 82.00 | 5.27 | 16.70 | 86.68 | 25.00 | 401.00 | 340.50 | 7.50 |
| Average | 61.78 | 0.54 | 50.89 | 2.61 | 7.85 | 30.33 | 10.92 | 205.23 | 211.61 | 5.57 |
| Standard deviation | 26.94 | 0.19 | 18.68 | 0.97 | 2.70 | 17.37 | 5.50 | 84.90 | 75.43 | 0.56 |

## 3 Analysis of influence factors of TBM rock mass boreability

The boreability of TBM rock mass is related to many factors, such as rock strength, intactness degree of rock mass, rock joint plane occurrence, groundwater, ground stress and tunnel diameter[1]. In general, many scholars assume that among these factors, the uniaxial compressive strength, intactness degree of rock mass, and the angle between the main structural plane and the tunnel axis have the most significant influence on rock mass boreability. In the following section, these influence factors of boreability of TBM rock mass are discussed in detail based on the database.

### 3.1 Uniaxial compressive strength of rock

TBM disc cutter breaking rock consists of two separate stages: cutter penetrating rock mass and rock fragments formation. A crushed zone occurs when the invasive load reaches the compressive strength of the rock, creating radial, central, and lateral cracks. These cracks propagate continuously along with the penetration of disc cutter. Eventually, rock fragments are formed when the cracks propagate to the surface or connect to other cracks resulted from adjacent cutters[31]. Therefore, the compressive strength of rock is remarkably correlated with the boreability of TBM rock mass. With the increase of rock compressive strength, the load required for cutter penetration increases, the rock mass boreability deteriorates, and the FPI gradually increases. As the compressive strength of rock decreases, it is more conducive to break rock by cutters. Consequently, the rock mass boreability is enhanced and FPI value goes down (Fig. 3). It is worth noting that, in Fig. 3, the rock mass boreability documented from different projects varies significantly with the varia- tion of uniaxial compressive strength of the rock. With the increase of tunnel diameter, FPI increases evidently with the increase of UCS. So it can be inferred that tunnel diameter $D$ may also have certain impact on the boreability of TBM rock mass.

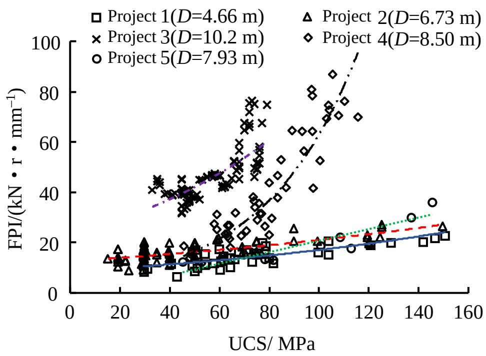


**Fig.3 Relationship between UCS and FPI**

### 3.2 Intactness degree of rock mass

In general, the poorer the intactness of the rock mass, the more developed its joints. Based on the above mechanism of TBM disc cutter rock breaking, the existence of joints facilitates cracks propagation in the process of rock breaking, which is favorable for the formation of rock fragments and improves the TBM tunneling efficiency[11]. Therefore, with the increase of the intactness degree of rock masses $K_{\text{v}}$, the FPI increases, and the boreability of TBM rock mass deteriorates gradually (Fig.4). However, an abnormal trend in Project 3 (West Qinling Tunnel of Lanzhou–Chongqing Railway ) is encountered that for broken rock masses, FPI decreases with the increase of $K_{\text{v}}$. This maybe because of the relatively high uniaxial compressive strength for the broken rocks (Fig.5), since the boreability of TBM rock mass is determined by both uniaxial compressive strength and intactness degree of rock masses. In addition, compared with small diameter tunnels, the increase of FPI with $K_{\text{v}}$ is faster in large diameter tunnels. Therefore, it can be inferred that there may be coupling effects among the influencing factors of rock mass boreability, which should be paid attention to during the establish- ment of the empirical prediction model for TBM rock mass boreability.

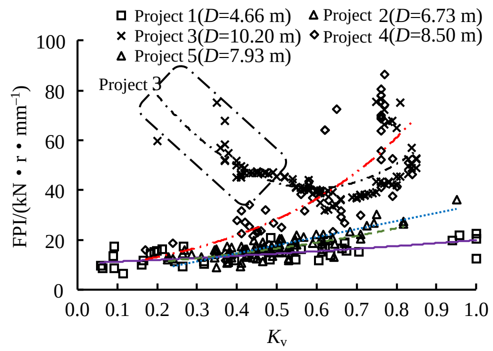


**Fig.4 Relationship between $K_{\text{v}}$ and FPI**

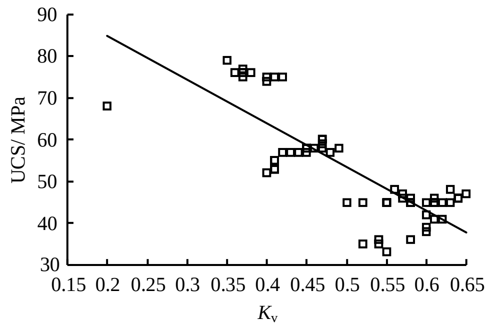


**Fig.5 Relationship between $K_{\text{v}}$ and UCS of project 3**

### 3.3 Angle between the main structural plane and tunnel axis

The angle between the main structural plane and tunnel axis, $\alpha$, also has significant impact upon TBM rock mass boreability. At a smaller $\alpha$ value, the cracks propagate from the invading position to the original structural plane during the TBM tunneling, whereas the cracks propagate from the original structural plane to the invading position at a larger $\alpha$ value[32]. With $\alpha$ decreases, the original structural plane will trigger the cracks to propagate into the deep of the rock, which is unfavourable for rock breaking. However, under a larger $\alpha$ value, the original structural plane would induce the cracks to propagate laterally, facilitateing the formation of rock fragments, although the large pieces of rock masses adversely affect the efficiency of rock breaking[33]. As a consequence, the boreability of rock mass is enhanced first and then deteriorates with the successive increase of $\alpha$. An optimized boreability of rock mass occurs when $\alpha$ ranges from 40° to 70° (Fig.6).

### 3.4 Tunnel diameter

The above analysis indicates that the TBM rock mass boreability difffers greatly with the variation of rock mass parameters (UCS, $K_{\text{v}}$, $\alpha$) for different diameter tunnels. The reason is for large diameter TBM tunneling, the resistance resulted from rock breaking becomes higher. Under the same stress state, the penetration distance in each turn is less than that of the small diameter TBM tunneling[1], leading to a degraded boreability for large diameter TBM tunneling. Given this situation, the relation between FPI and tunnel diameter *D* is obtained based on the data in the database (Fig. 7). As depicted in Fig. 7, FPI increases exponentially with increasing tunnel diameters. Thus, tunnel diameter *D* is also an critical factor in the establishment of empirical prediction model of TBM rock mass boreability.

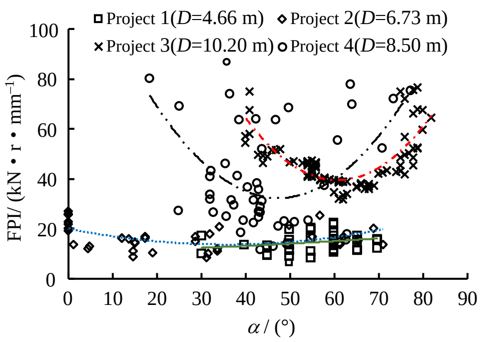


**Fig.6 Relationships between $\alpha$ and FPI**

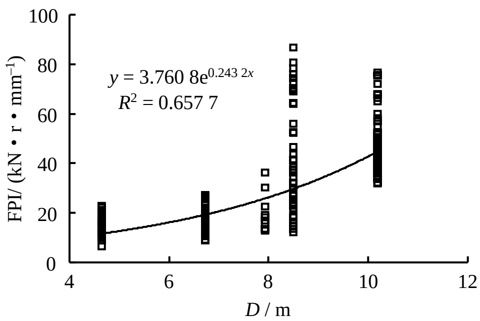


**Fig.7 Influence of tunnel diameter on boreability of rock mass**

## 4 Empirical prediction method of TBM rock mass boreability

The above analysis suggests that rock uniaxial compressive strength, intactness degree of rock masses, angle between main structural plane and tunnel axis, and tunnel diameter all have significant influences on the boreability of TBM rock mass. In this study, UCS, $K_v$, $\alpha$, and *D* are taken as independent variables and the rock mass boreability evaluation index FPI is treated as a dependent variable. SPSS software is used for nonlinear regression analysis to establish the empirical prediction method of TBM rock mass boreability. Through a series of mathematical modeling analysis, it is found that the prediction method yields an optimized result when the influence of the angle between the main structural plane and tunnel axis is not considered. The mathematical model is expressed as follows:

$$\mathrm{FPI} = \mathrm{e}^{a_1 D}(a_2 \mathrm{UCS}^{a_3} \mathrm{e}^{a_4 K_v} + a_5) \quad (4)$$

where $a_1$, $a_2$, $a_3$, $a_4$ and $a_5$ are regression parameters.

As aforementioned, the boreability of TBM rock mass deteriorates with the increase of UCS, $K_v$ and *D*. In order to ensure that the fitting results are consistent with practical judgment, the limitation of $a_1$ to $a_5$ in the regression process are listed in Table 5.

**Table 5 Initial conditions of model parameters**

| Regression parameters | $a_1$ | $a_2$ | $a_3$ | $a_4$ | $a_5$ |
|---|---|---|---|---|---|
| Limitation | ⩾0 | ⩾0 | ⩾0 | ⩾0 | 无 |

$$\mathrm{FPI} = \mathrm{e}^{0.287D}(0.004\mathrm{UCS}^{1.342}\mathrm{e}^{0.44K_v} + 1.25) \quad (5)$$

After regression fitting, the empirical prediction formula of boreability is obtained:

$$\mathrm{FPI} = \mathrm{e}^{0.287D}(0.004\mathrm{UCS}^{1.342}\mathrm{e}^{0.44K_v} + 1.25) \quad (5)$$

In this formula, FPI increases with the increase of tunnel diameter, rock uniaxial compressive strength and intactness degree of rock masses. Meanwhile, there is an obvious coupling effect between these three factors, which is consistent with the above discussion. The comparison results between the measured FPI and the predicted FPI are shown in Fig. 8. The correlation coefficient between the predicted results and the measured results is about 0.768 with an acceptable deviation, indicating that this empirical method can be applied confidently to predict the boreability of TBM rock mass.

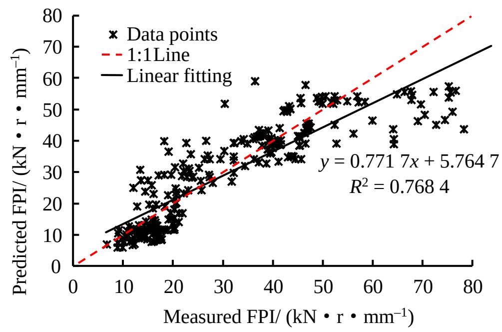


**Fig.8 Comparison between measured FPI and predicted FPI**

## 5 Classification of TBM rock mass boreability

During the practical construction process, with the change of TBM rock mass boreability, the TBM tunneling parameters should also be adjusted timely to realize safe and efficient tunneling, among which the thrust of disc cutter and its rotational speed are the core controlling parameters. Given the differences in the machinery installed size, the number of disc cutters, and the installed powers for different TBM, the average utilization rate of the thrust of single cutter and disc cutters rotational speed are chosen as the controlling parameters of TBM tunneling, so as to further explore the relationship between these parameters and rock mass boreability. The cutter thrust and rotational speed can be obtained in the practical engineering cases by combing the conversion of mechanical parameters, which are presented as

$$U_F = \frac{F_n}{F_{nmax}} \times 100\% \qquad (6)$$

$$U_R = \frac{RPM}{RPM_{max}} \times 100\% \qquad (7)$$

where $U_F$ is the utilization ratio of the average thrust of single cutter(%); $F_{n max}$ is the maximum average thrust of single cutter(kN); $U_R$ is the utilization rate of cutterhead rotational speed(%); RPM is real cutterhead rotational speed(r/min); and $RPM_{max}$ is the maximum cutterhead rotational speed(r/min).

Based on the above analysis, FPI is selected as the classification index for rock mass boreability. Taking into account the differences of TBM tunneling parameters selection under different rock mass boreability conditions in the practical engineering projects, we choose FPI, $U_F$ and $U_R$ as cluster variables to carry out the rock mass boreability classification. Based on the valid data containing FPI, $U_F$ and $U_R$ in the database, K-center clustering method was implemented using SPSS software. Referring to the existing research results of boreability classification of TBM rock mass[2, 5, 12], the number of classification is specified as 6 to conduct iterative classification. The *F* test of the results is shown in Table 6. *P* values of all cluster variables are small, indicating the validity of this classification method. Figure 9(a) describes the FPI value corresponding to each group of rock mass. There is no overlap between the FPI of each group, indicating that it is appropriate to take FPI as the rock mass classification index. The specific classification results are shown in Table 7. The smaller the *P* value, the more likely the rock is to be broken. For the surrounding rocks, from B–I to B–VI, the boreability of rock mass deteriorates successively with the resistance of TBM tunneling increasing. The surrounding rocks in the database are grouped in Fig.9 (b), in which B–V,B–VI surrounding rocks occupy a small proportion, indicating that most of the surrounding rock sections involved in the database are inclined to be tunneled easily.

**Table 6 A F-test of the clustering results**

| Clustering variables | Clustering results: Mean square error | Clustering results: df | Error: Mean square error | Error: df | F test | *P* |
|---|---|---|---|---|---|---|
| FPI | 12 744.953 | 5 | 8.695 | 248 | 1 465.863 | 0.00 |
| $U_F$ | 5.909 | 5 | 0.019 | 248 | 314.768 | 0.00 |
| $U_R$ | 0.458 | 5 | 0.005 | 170 | 94.245 | 0.00 |

Note: df is the degree of freedom and *P* is the significance level.

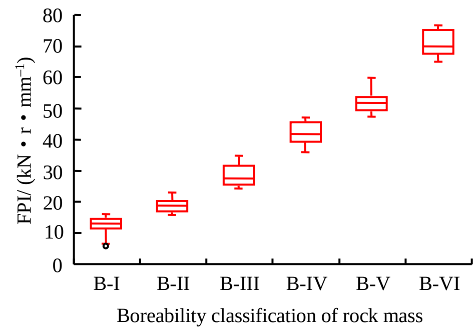


(a) FPI value for each group of rock mass

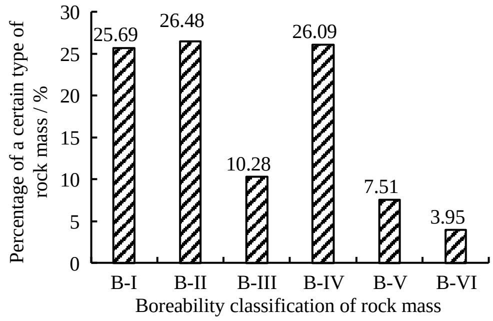


(b) Distribution of each group of rock mass

**Fig.9 Rock mass boreability classification**

**Table 7 Rock mass boreability classification in TBM tunnel**

| Classification of rock mass boreability | FPI / (kN • r • mm$^{-1}$) | Suggested $U_F$ value | Suggested $U_R$ value |
|---|---|---|---|
| B-I | <16 | 22.7% | 59.8% |
| B-II | 16–24 | 0.037FPI – 0.406 | $\frac{1}{1+e^{-0.13FPI+1.89}}$ |
| B-III | 24–36 | 0.037FPI – 0.406 | $\frac{1}{1+e^{-0.13FPI+1.89}}$ |
| B-IV | 36–48 | 98.1% | 86.8% |
| B-V | 48–64 | 98.1% | 86.8% |
| B-VI | >64 | 98.1% | 86.8% |

Note: $FPI = e^{0.287D}(0.004UCS^{1.342}e^{0.44K_v} + 1.25)$

Based on the data in the database, the relationships between the utilization rate of average single cutter thrust, the utilization ratio of cutterhead rotational speed and rock mass boreability can be achieved, as plotted in Fig. 10 and Fig. 11. In terms of the easy broken surrounding rock, such as B–I, the rock strength is relatively low, and the intactness and stability of rock mass are inferior. In order to ensure the safety of construction, low tunneling parameters are commonly adopted. To be specific, the average single cutter thrust efficiency is about 20%, and the utilization ratio of disc cutter rotational speed is about 60%. However, due to the distinction of the stability of surrounding rocks and the experience of the TBM operators, the selection of tunneling parameters tend to have larger discreteness. With the increase of FPI, rock mass boreability deteriorates evidently. In order to realize effective TBM rock breaking, in B–II and B–III surrounding rocks, TBM operators used to increase the tunneling parameters. Therefore the utilization ratio of average single cutter thrust and cutterhead rotational speed increase with the increase of FPI. For B–IV, B–V and B–VI groups of surrounding rocks, the rock mass is relatively stable. To achieve an acceptable penetration rate, TBM operators take the initiative to adjust tunneling parameters value close to the upper limit. Specifically, the average single cutter thrust efficiency approaches 100%, and the utilization ratio of disc cutter rotational speed is around 90%. Nevertheless, in Fig.10, the lower $U_F$ in B–IV, B–V and B–VI surrounding rocks is due to the excessive groundwater flux in the corresponding tunneling sec- tions in Project 3 (West Qinling tunnel of Lanzhou– Chongqing Railway) (Fig.12). In order to guarantee the safety of the TBM construction, TBM operators reduced the thrust of cutterhead to meet the safety requirements of TBM construction.

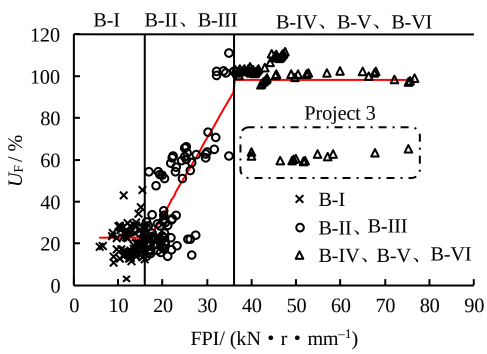


**Fig.10 Relationship between the $U_F$ and FPI**

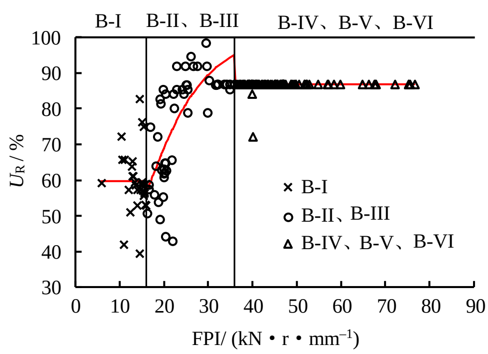


**Fig.11 Relationship between $U_R$ and FPI**

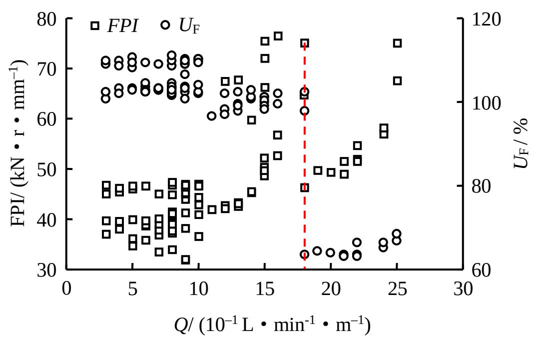


**Fig.12 Influence of underground water on $U_F$ in project 3**

Based on the discussion above, a classification table (Table 7) of the boreability of TBM tunnel rock mass can be obtained, which has guiding significance in the evaluation of TBM rock mass boreability and the selection of tunneling parameters.

The relationship between TBM net penetration rate, PR and field penetration index, FPI is given by

$$PR = \frac{60RPM \cdot F_n}{1\ 000FPI} = \frac{60U_R U_F}{1\ 000FPI} RPM_{max} F_{n\,max} \tag{8}$$

Using the classification table, the TBM penetration rate of Project 3 (West Qinling tunnel of Lanzhou–Chongqing railway) and Project 4 (A typical water diversion tunnel) in the database can be predicted (Fig. 13). It can be found that the measured PRs in Project 3 and Project 4 agree well with the predicted PRs, while part of the measured PRs in Project 3 are significantly lower than the predicted PRs, which is caused by the excessive groundwater flux in the tunnel sections and the reduction of the thrust of cutterhead by TBM operators. Therefore, the results highlight that the rock mass boreability classification table proposed in this study is of practicability. This classification table can be used to preliminarily predict the net penetration rate of TBM and guide the arrangement of construction schedule.

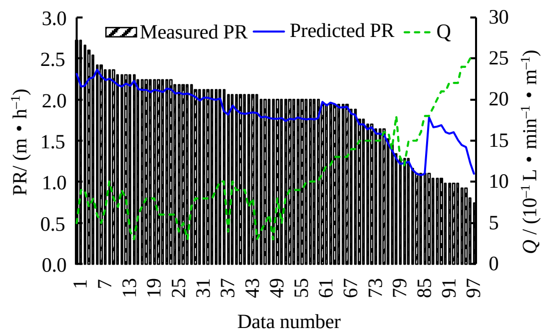


(a) West Qinling tunnel of Lanzhou–Chongqing Railway (Project 3)

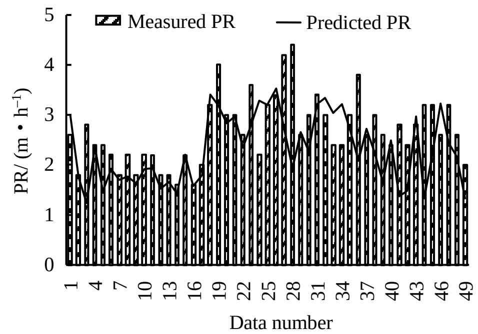


(b) A typical water diversion tunnel (Project 4)

**Fig.13 The comparison between measured PR and predicted PR**

In practical engineering projects, it is advisable to combine the above empirical formula with the field data to calculate the FPI value, so as to perform classification of the boreability of TBM rock mass and guide the selection of tunneling parameters ($U_F$ and $U_R$ ), and eventually guide the arrangement of construction schedule. It should be noted that the selection of TBM tunneling parameters is affected by the rock mass boreability, stability, operators' experiences and other factors. This paper provides a suggested value of tunneling parameters in view of rock mass boreability. The parameter selection and construction schedule should be adjusted appropriately according to the practical tunneling settings.

## 6 Discussion

(1) This study is based on the measured data from different engineering projects. In order to characterize the different parameters of an specified property of rock mass, RQD is converted to $K_v$. The correlations between RQD or $K_v$ and FPI are identical to each other. The results reveal that this conversion method is suitable for the study of TBM rock mass boreability. But because of the lack of the validation by measured data, the applicability of the conversion method in other fields need to be inspected carefully.

(2) In this study, field penetration index, FPI is adopted to evaluate the boreability of TBM rock mass. Although it can eliminate the influence of single cutter thrust and penetrating distance per turn of disc cutter, it is still affected by other mechanical parameters. In subsequent studies, a more suitable evaluation index for the boreability of TBM rock mass should be proposed as far as possible.

(3) The boreability of TBM rock mass is affected by many factors. Due to the limitation of data coverage, this paper only discusses the influences of tunnel diameter, rock uniaxial compressive strength, intactness degree of rock masses and main structural plane of rock mass, as well as the coupling effects among these factors. In fact, other factors, such as groundwater condition, in-situ stress state, rock brittleness also exert certain impacts on rock mass boreability, which should be studied via combining with corresponding field measured data.

(4) The database is the basis of the empirical predicttion method of TBM rock mass boreability proposed in this study. It covers the measured data from TBM constructions in igneous rock, sedimentary rock and metamorphic rock. Though its applicability is relatively extensive, we should also be aware of the limitations of this empirical method since it seems to be site-specific. In order to improve the applicability of the empirical method, more measured data from different lithology should be collected for the establishment of the prediction model.

(5) The classification of TBM rock mass boreability and the suggested TBM tunneling parameters are mainly based on the data in the database, hence it can be used as reference in practical engineering operations. However, it is imperative to combine with the practical construction conditions closely since the tunneling parameters are determined by many factors such as the boreability of rock mass, the stability of surrounding rock and the experiences of TBM operators.

## 7 Conclusions

Based on the field measured tunneling data, rock mass parameters and boreability evaluation index for different types of rock and TBM, the influencing factors for TBM rock mass boreability were analyzed comprehensively. An empirical prediction method of boreability and a systematic classification scheme were proposed. The main conclusions can be drawn as follows:

(1) The boreability of TBM rock mass is influenced by many factors. Based on the collected data, it is found that a strong rock uniaxial compressive strength, a high intactness degree of the rock mass and an enlarged tunnel diameter usually correspond to a poor boreability. With the increase of the angle between the main structural plane and tunnel axis, the boreability experiences a upgrade first, followed by a downward trend. The coupling impacts of various factors on the rock mass boreability are also witnessed.

(2) In this paper, FPI is selected as the evaluation index of rock mass boreability, and the established prediction formula is $\mathrm{FPI} = \mathrm{e}^{0.287D}(0.004\mathrm{UCS}^{1.342} \cdot \mathrm{e}^{0.44K_v} + 1.25)$, which is consistent with professional judgment. The correlation coefficient between the predicted results and the measured results is about 0.768 with an acceptable deviation, indicating a satisfying prediction effect.

(3) Based on the proposed empirical prediction method, the boreability of rock mass can be divided into 6 categories. With the deterioration of the boreability of rock mass, TBM operators often adopt higher tunneling parameters to achieve the appropriate TBM penetration rate. The proposed values of TBM tunneling parameters under different rock mass boreability conditions can be used as a reference for practical engineering projects. Based on the relationship between tunneling parameters and rock mass boreability, the preliminary prediction of TBM penetration rate can be conducted, which provides guidance for the arrangement of TBM construction schedule.

### Reference

[1] LIU Quan-sheng, LIU Jian-ping, PAN Yu-cong, et al. Research advances of tunnel boring machine performance prediction models for hard rock[J]. Chinese Journal of Rock Mechanics and Engineering, 2016, 35(Suppl.1): 2766–2786.

[2] XUE Ya-dong, LI Xing, DIAO Zhen-xing, et al. A novel classification method of rock mass for TBM tunnel based on penetration performance[J]. Chinese Journal of Rock Mechanics and Engineering, 2018, 37(Suppl.1): 3382–3391.

[3] WANG Xu, LI Xiao, LI Shou-ding. Problems in the prediction of the TBM advance rate with rock mass classification and their possible solutions[J]. Journal of Engneering Geology, 2008, 16(4): 470–475.

[4] GONG Q, YIN L, MA H, et al. TBM tunnelling under adverse geological conditions: an overview[J]. Tunnelling and Underground Space Technology, 2016, 57: 4–17.

[5] DU Li-jie, QI Zhi-chong, HAN Xiao-liang, et al. Prediction method for the boreability and performance of hard rock TBM based on boring data on site[J] Journal of China Coal Society, 2015, 40(6): 1284–1289.

[6] KHADEMI HAMIDI J, SHAHRIAR K, REZAI B, et al. Performance prediction of hard rock TBM using rock mass rating (RMR) system[J]. Tunnelling and Underground Space Technology, 2010, 25(4): 333–345.

[7] ROSTAMI J. Development of a force estimation model for rock fragmentation with disc cutters through theoretical modeling and physical measurement of crushed zone pressure[D]. Golden: Colorado School of Mines, 1977.

[8] BARTON N. Rock mass classification for choosing between TBM and drill-and-blast or a hybrid solution[C]// Proceedings Internation Conference on Tunnels and Underground Structures. Singapore: [s. n.], 2000: 35-50.

[9] BARTON N. TBM tunnelling in jointed and faulted rock[M]. Boca Raton: CRC Press, 2000.

[10] CASSINELLI F, CINA S, INNAURATO N. Power consumption and metal wear in tunnel-boring machines: analysis of tunnel-boring operation in hard rock[C]// Proceedings of the 3rd International Symposium. Brighton: [s. n.], 1982: 73–81.

[11] YAGIZ S. Utilizing rock mass properties for predicting TBM performance in hard rock condition[J]. Tunnelling and Underground Space Technology, 2008, 23(3): 326–339.

[12] HASSANPOUR J, ROSTAMI J, ZHAO J. A new hard rock TBM performance prediction model for project planning[J]. Tunnelling and Underground Space Technology, 2011, 26(5): 595–603.

[13] HASSANPOUR J, A. GHAEDI VANANI A, ROSTAMI J, et al. Evaluation of common TBM performance prediction models based on field data from the second lot of Zagros water conveyance tunnel (ZWCT2)[J]. Tunnelling and Underground Space Technology, 2016, 52: 147–156.

[14] HASSANPOUR J, ROSTAMI J, KHAMEHCHIYAN M, et al. Developing new equations for TBM performance prediction in carbonate-argillaceous rocks: a case history of Nowsood water conveyance tunnel[J]. Geomechanics and Geoengineering, 2009, 4(4): 287–297.

[15] HASSANPOUR J, ROSTAMI J, KHAMEHCHIYAN M, et al. TBM performance analysis in pyroclastic rocks: a case history of Karaj water conveyance tunnel[J]. Rock Mechanics and Rock Engineering, 2010, 43(4): 427–445.

[16] LIU Q, LIU J, PAN Y, et al. A case study of TBM performance prediction using a Chinese rock mass classification system – hydropower classification (HC) method[J]. Tunnelling and Underground Space Technology, 2017, 65: 140–154.

[17] HASSANPOUR J, ROSTAMI J, ZHAO J, et al. TBM performance and disc cutter wear prediction based on ten years experience of TBM tunnelling in Iran[J]. Geomechanics and Tunnelling, 2015, 8(3): 239–247.

[18] QI Zhi-chong. Researches on open TBM geology adaptability and construction technology[D]. Shijiazhuang: Shijiazhuang Tiedao Univercity, 2015.

[19] BRULAND A. Hard rock tunnel boring[D]. Trondheim: Norwegian University of Science and Technology, 1998.

[20] FROUGH O, TORABI S R, TAJIK M. Evaluation of TBM utilization using rock mass rating system: a case study of Karaj-Tehran water conveyance tunnel (lots 1 and 2)[J]. Journal of Mining & Environment, 2012, 3(2): 89–98.

[21] WANG Pan. Research on penetrability prediction analysis method of tunneling boring machine[D]. Tianjin: Tianjin University, 2014.

[22] WANG Pan, GUO Wei, ZHU Dian-hua. A prediction model of boreability of surrounding rock in TBM construction based on fuzzy clustering theory[J]. Modern Tunnelling Technology, 2014(6): 58–65.

[23] ZHAO Zhan-xin. Wear analysis of TBM disc cutter in West Qinling super long tunnel[J]. Construction Mechanization, 2014(1): 79–81.

[24] LI Nan-chuan. TBM stepping technology: case study on West Qinling tunnel[J]. Tunnel Construction, 2011(6): 749–754.

[25] WANG Jian, WANG Rui-hui, ZHANG Xin-xin, et al. Estimation of TBM performance parameters based on rock mass rating (RMR) system[J]. Tunnel Construction, 2017(6): 700–707.

[26] HAMILTON W, DOLLINGER G. Optimizing tunnel boring machine and cutter design for greater boreability[C]//Proceedings of the Rapid Excavation and Tunneling Conference. Atlanta: [s. n.], 1979: 280–296.

[27] MA Chao-feng, LI Xiao, CHENG Guo-wen, et al. Study of practical approach to assess integrality of engineering rock mass[J]. Rock and Soil Mechanics, 2010, 31(11): 3579–3584.

[28] ZHOU Shu-da, PEI Qi-tao, DING Xiu-li. Application of grey evaluation model based on classification degree and weight of classification of index to rock mass quality evaluation of underground engineering[J]. Chinese Journal of Rock Mechanics and Engineering, 2016, 35(Suppl.2): 3671–3679.

[29] WANG Jia-xin, ZHOU Zong-hong, ZHAO Ting, et al. Application of Alpha stable distribution probabilistic neural network to classification of surrounding rock stability assessment[J]. Rock and Soil Mechanics, 2016, 37(Suppl.2): 649–657, 664.

[30] Ministry of Construction, the People's Republic of China. GB50021－2001 Geotechnical survey specification[S]. Beijing: China Architecture and Building Press, 2009.

[31] GONG Qiu-ming. Introduction of TBM tunnelling[M]. Beijing: Science Press, 2014.

[32] BEJARI H, KHADEMI HAMIDI J. Simultaneous effects of joint spacing and orientation on TBM cutting efficiency in jointed rock masses[J]. Rock Mechanics and Rock Engineering, 2013, 46(4): 897–907.

[33] SUN Jin-shan, CHEN Ming, CHEN Bao-guo, et al. Numerical simulaiton of influence factors for rock fragmentation by TBM cutters[J]. Rock and Soil Mechanics, 2011, 32(6): 1891-1897.